frontiers | Frontiers in Energy Research

TYPE Original Research
PUBLISHED 29 December 2023
DOI 10.3389/fenrg.2023.1328662

OPEN ACCESS

EDITED BY
Xiaojin Zheng,
Princeton University, United States

REVIEWED BY
Wang Song,
China University of Petroleum, China
Bo Yu,
Northeast Petroleum University, China

*CORRESPONDENCE
Li Dan,
lidan6@cnooc.com.cn

RECEIVED 27 October 2023
ACCEPTED 29 November 2023
PUBLISHED 29 December 2023

CITATION
Yu Q, Dan L, Shanshan Y and Qixin L (2023), Geophysical exploration methods on bauxite reservoirs in L gasfield, Ordos Basin.
Front. Energy Res. 11:1328662.
doi: 10.3389/fenrg.2023.1328662

Geophysical exploration methods on bauxite reservoirs in L gasfield, Ordos Basin

Qi Yu, Li Dan*, Yu Shanshan and Li Qixin

Cnooc Research Institute Ltd., Beijing, China

Introduction: The L gasfield on the eastern edge of the Ordos Basin mainly focuses on the exploration and development of coalbed methane and tight sandstone gas. As the overlying strata of Majiagou Formation of Lower Ordovician in Lower Paleozoic, bauxite has always been considered a regional cap rock and has not been widely followed with interest. The drilled wells has revealed that bauxite can be used as a unconventional reservoir with good reservoir properties. In the future, it will become a new natural gas exploration target in the L region. This article is dedicated to the comprehensive study of geophysical methods for the bauxite exploration in the L region.

Methods: Firstly, we use seismic data to restore paleo-geomorphology of the Lower Paleozoic. Secondly, we analyze the well log data of different paleo-geomorphic unit. Then, we establish a mineral model based on the logging data to calculate the lithological composition and porosity, and use imaging logging to evaluate the pore structure and fluid type.

Result and Discussion: Finally, we obtained favorable reservoir development zones for bauxite, guiding exploration and evaluation of bauxite.

KEYWORDS

bauxite reservoirs, paleo-geomorphology, well logging evaluation, imaging logging, unconventional reservoir

1 Introduction

The L region is an unconventional gas region of China National Offshore Oil Corporation. Mainly focused on the exploration and development of tight sandstone gas and deep coalbed methane in the Carboniferous and Permian. At present, exploration in these two fields has gradually come to an end (Zhu et al., 2022; FengRuyong, 2022; Li, 2023; Xu et al., 2023; Tang et al., 2022; Tang et al., 2023). In the L region, as the overlying strata of Ordovician in Lower Paleozoic, bauxite has always been considered a regional cap rock and has not been widely followed with interest (Nan et al., 2022; Pan et al., 2023; Yuan et al., 2016). After 2020, China National Petroleum Corporation Changqing Oilfield conducted research and production testing on bauxite reservoirs, obtaining high production. During this period, She, Du, and others conducted geophysical forward modeling research on the sedimentary structure of bauxite, and used waveform indication simulation technology and inversion to predict the reservoir of bauxite (She et al., 2022; Du et al., 2022). Liu Wenhui and others qualitatively evaluated bauxite reservoirs using conventional, Full Micro-Resistivity Imaging (FMI) and Nuclear Magnetic Resonance (NMR) logging (Liu et al., 2015; Liu et al., 2022a). Liu Die quantitatively explained the lithology and porosity of bauxite reservoirs through core experimental data, combined with conventional logging and imaging logging (Liu et al., 2022b). Fu Jinhua conducted a detailed

analysis of nearly a hundred rock samples from the bauxite formation, and concluded that the bauxite reservoir developed dissolution pores and was controlled by sedimentary paleo-environments and paleo-geomorphology. The conclusion was drawn that bauxite gas exploration has opened up new fields for basin exploration (Fu et al., 2021; Fu et al., 2023). Comprehensive research has revealed that bauxite has become a new unconventional reservoir, but the exploration techniques for bauxite in different regions vary, and it is still necessary to find suitable exploration techniques for us.

This article uses 3D seismic data and logging data from nearly 160 drilled wells to restore paleo-geomorphology using the impression method, and obtains a map of the Ordovician top interface paleo-geomorphology. We classified and analyzed the bauxite rock data under different karst backgrounds. Establish a quantitative evaluation method for logging in this region through existing core experiments, and analyze the pore structure in combination with ERMI and NMR logging. Conduct a detailed analysis of the drilling data from over a hundred existing wells in this area to guide the exploration and development of bauxite suitable for this region.

2 Regional overview

The region L is located in the eastern edge of the Ordos Basin. The main exploration targets are the Upper Paleozoic Carboniferous Benxi Formation, Permian Shihezi Formation, Shanxi Formation, and Taiyuan Formation. Among them, the 4 + 5$^{\#}$ and 8 + 9$^{\#}$ coal seams developed in the Benxi Formation and Taiyuan Formation are the main source rocks. The tight sandstone reservoirs of the Upper Paleozoic in this area belong to typical lithological gas reservoirs. Influenced by the Northern source and sedimentary environment, shallow marine delta or shallow lake delta sand bodies are mainly developed. Currently, the main exploration and development forces are still tight sandstone gas and deep coalbed methane.

The bauxite rock is developed at the bottom of the Benxi Formation and is a product of the weathering crust karst deposition of the Lower Paleozoic Ordovician. The Benxi Formation in the eastern part of the Ordos Basin is mainly composed of shallow sea continental shelves, lagoons, and tidal flats. A set of strata composed of iron aluminum layers, mudstones, sandstones, limestone, and coal seams was deposited. The lagoon facies developed gray black iron aluminum mudstone, bauxite, and tuffaceous sandstone and mudstone.

Bauxite rock is formed by weathering and leaching of aluminosilicate minerals in the original rock, forming aluminum containing colloids and high potassium clay. It is transported *in situ* or close proximity to karst depressions, lakes, bays, and lagoon basins, and is directly deposited or formed by terrestrial decomposition, directly covering the weathered crust, forming characteristic oolitic, bean and block structures.

3 Reservoir characteristics and exploration research methods of bauxite

The bauxite in China can be divided into four types: sedimentary type, accumulation type, laterite type, and magmatic type. The bauxite in this study belongs to the weathering crust sedimentary type. The underlying bedrock is Ordovician carbonate rock. Due to different weathering crust karst processes, the sedimentary thickness of bauxite varies greatly and is widely distributed. Under different sedimentary conditions, the thickness, mineral content, and porosity of bauxite varies. At present, bauxite rock settlement can be divided into three categories: monadnock, terraces, and trenches. By using paleo-geomorphic restoration techniques, these three types of sedimentary methods can be accurately classified.

The main mineral of bauxite is diaspore, which can be divided into bauxite mudstone (with a diaspore content of 25%–50%), argillaceous bauxite (with a diaspore content of 50%–75%), and bauxite (with a diaspore content exceeding 75%) based on its mineral content. Through X-Ray Diffraction (XRD) analysis, in addition to diaspore, bauxite contains terrigenous clastic rocks such as clay minerals and quartz, as well as heavy minerals such as pyrite, hematite, and anatase. The mineral composition is complex and diverse (Table 1). The highest content of diaspore is 94%, the highest content of heavy metals is 35%, and the clay minerals range from 3% to 10%, with a porosity range of 2.5%–10%.

The logging of bauxite have the characteristics, which are high neutron, high gamma, high density, low slowness and low resistivity. Under weathering and leaching, elements such as potassium and sodium are lost. During the Ordovician period, the Ordos Basin was at a high tide of marine invasion, and the crust continued to sink during the sedimentary period of the Benxi Formation, further expanding the scope of marine invasion. The abundance of carbonate solution increases the solubility of uranium in seawater, and elements such as uranium and thorium are transported and enriched after being fully analyzed. Bauxite rock have strong adsorption properties, resulting in the occurrence of high uranium, high thorium, and low potassium in the bauxite rock (Yang et al., 2006; Jiang and Wang, 2004). Enriched high radioactive elements such as uranium and thorium result in abnormally high natural gamma rays, with some layers having natural gamma values higher than 600API.Therefore, using gamma rays to determine the formation of bauxite has become the most commonly used logging method.

The exploration technology and methods for bauxite reservoirs, which detailed introduction in Figure 1, are mainly divided into the following three steps:1) Using a large amount of drilled data and 3D seismic data, the Paleo-geomorphology restoration of the Ordovician top interface was carried out using impression technology.2) Establish a quantitative logging interpretation model based on core experimental data (XRD, physical property analysis, thin sections, etc.). Calculate parameters such as lithology, minerals, porosity, permeability, and divide pore structure through imaging logging system.3) Divide favorable areas for bauxite exploration through sedimentary characteristics and quantitative interpretation of drilled holes, and guide the next step of work.

4 Paleo-geomorphology restoration technology

The characteristics of Paleo-geomorphology control the mode and intensity of karst. The sedimentary characteristics of bauxite vary under different karst Paleo-geomorphology. This study used the impression method to restore Paleo-geomorphologys in the region.

TABLE 1 Mineral content and logging response table for core experiments.

Well	Lithology	Mineral content					Well log data				
		Diaspore	Sand	Shale	Pyrite	Anatase	GRAPI	DT us/ft	DEN g/cm3	$\varnothing_{cnl}$%	RtΩ·m
L-A	Argillaceous bauxite	71	2	7	4	13	497.4	59.0	2.97	56.8	199.6
L-A	Bauxite	80	0	6	6	12	546.5	52.5	3.15	67.5	22.4
L-A	Argillaceous bauxite	63	0	16	10	26	462.5	52.1	3.16	64.1	33.8
L-A	bauxitic shale	48	0	22	13	35	437.9	49.4	3.09	53.9	21.3
L-B	Bauxite	94	0	3	1	2	547.2	52.6	2.92	71.5	21.4

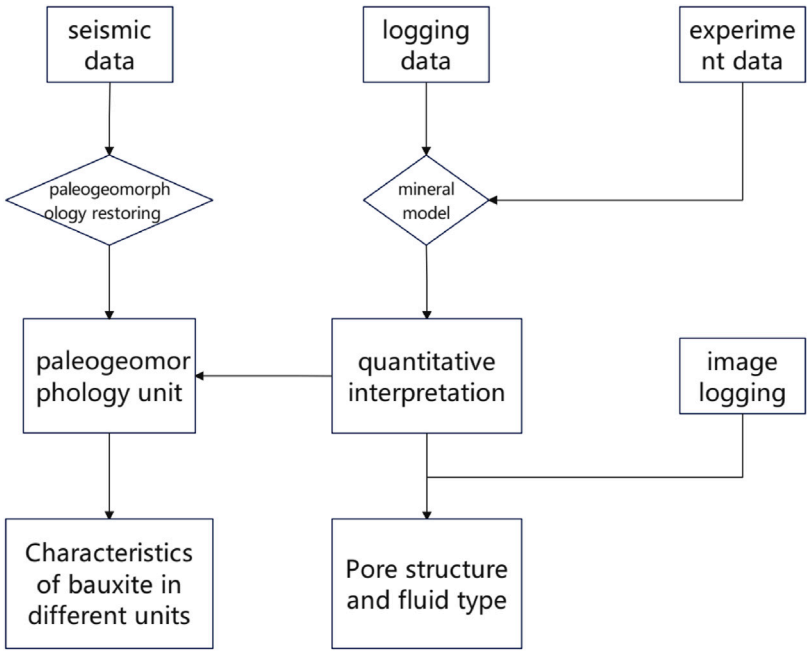

FIGURE 1
Flow chart of research on bauxite exploration methods.

The impression method utilizes the principle of sedimentary compensation to use the top boundary of the overlying strata as an isochronous reference plane, restoring the thickness between the top boundary of the erosion surface and the reference plane, and describing the paleo-geomorphology form through a mirror image relationship (Cao et al., 2020; Jia et al., 2023; Qiu et al., 2021). The top of the Benxi Formation is the 8# coal seam, which can be stably distributed and tracked throughout the entire area. The bottom of the Benxi Formation is the Ordovician erosion surface. By leveling the $8^{\#}$ coal seam, the bottom of the Benxi Formation is the pre-sedimentary Paleo-geomorphologys of Benxi.

4.1 Horizon interpretation

There is the stable coal seams in region at the top of Benxi formation, with a solid coal density of about 1.5 g/cm^3 and a sonic transit time of 120 us/ft, exhibiting low impedance and a strong amplitude trough in the seismic waveform, as shown in Figure 2. The bottom of Benxi is composed of bauxite and bauxite mudstone, and the underlying strata are Ordovician carbonate rocks. The density and velocity of bauxite vary with the content of diaspore. However, the underlying strata still exhibit high impedance, manifested as wave peaks, and the amplitude varies with the content of diaspore. The Benxi Formation is a transitional sedimentary facies of the sea route, with complex lithology, including various lithologies such as coal seams, sandstone, mudstone, limestone, bauxite.

As shown in Figure 3, according to more than 160 drilled wells in the region, the thickness of the Benxi Formation varies from 50 to 110 m. According to the thickness of the Benxi Formation, the Paleo-geomorphology units are further divided, as shown in Table 1. The lithology of the Benxi Formation includes coal and carbonaceous mudstone with low longitudinal impedance, mudstone with medium longitudinal

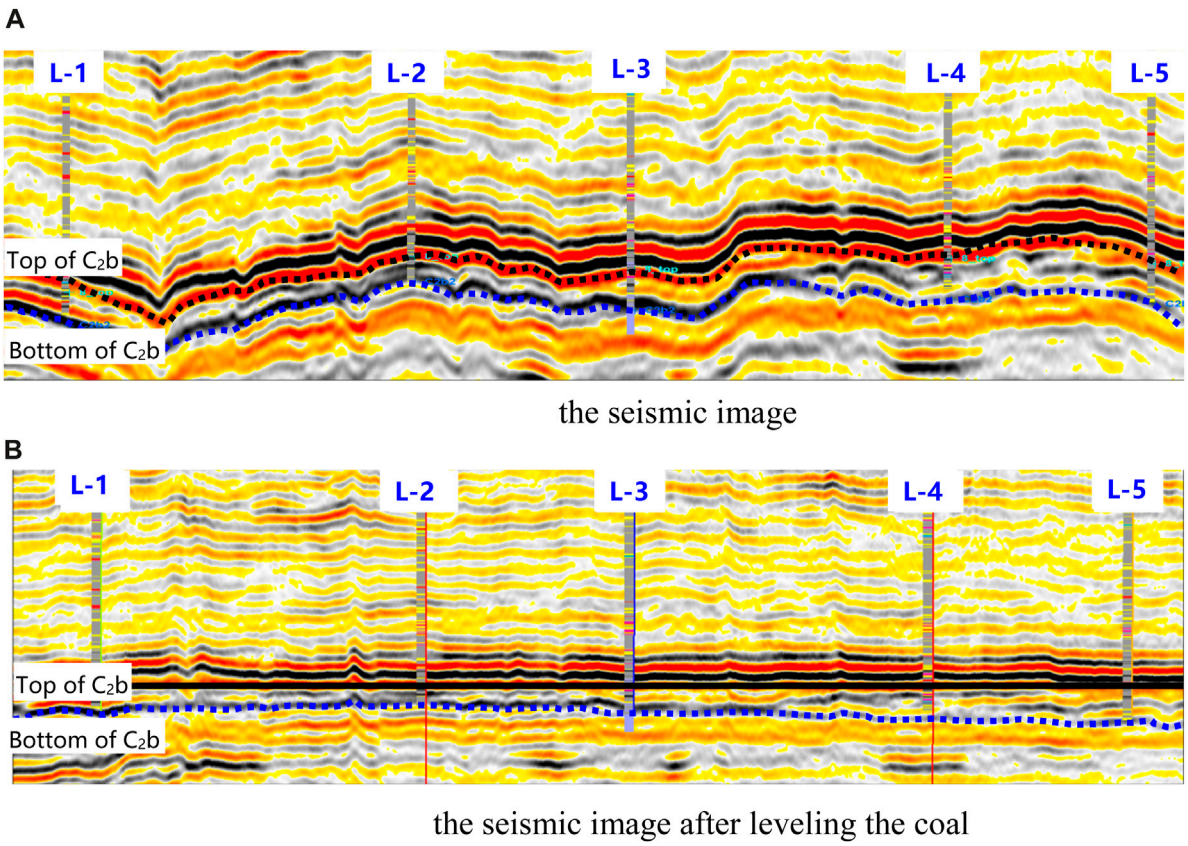

FIGURE 2
Impression method for paleo-geomorphology characterization. **(A)** the seismic image. **(B)** the seismic image after leveling the coal.

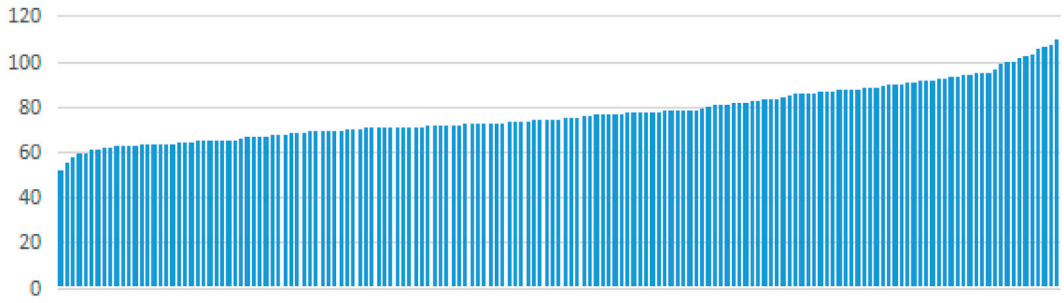

FIGURE 3
Thickness statistics of benxi formation for 162 Wells in L region.

impedance, gas-bearing sandstone, mudstone with medium to high longitudinal impedance, bauxite mudstone, dry sandstone, and limestone and bauxite with high longitudinal impedance. The complex and diverse lithology and wide range of thickness variation make it difficult to interpret the seismic horizons at the bottom of the Benxi Formation, This article verifies the correctness of the interpretation layers through forward modeling using different interpretation schemes.

4.2 Analysis of karst paleo-geomorphology classification

This region has been drilled and explained, with a depth range of 45–110 m in the Benxi Formation. As shown in Table 2, based on the thickness of the Benxi Formation and the classification of paleo-geomorphology, the secondary paleo-geomorphic units can be divided into karst slopes and karst

TABLE 2 Division table of paleo-geomorphic units.

Secondary paleo-geomorphic unit	Tertiary paleo-geomorphic unit	The thickness of benxi formation	
karst slopes	monadnock	45–90 m	45–55 m
	slopes		55–65 m
	trench		65–90 m
karst basins	monadnock	60–110 m	60–75 m
	terraces		75–85 m
	trench		85–110 m

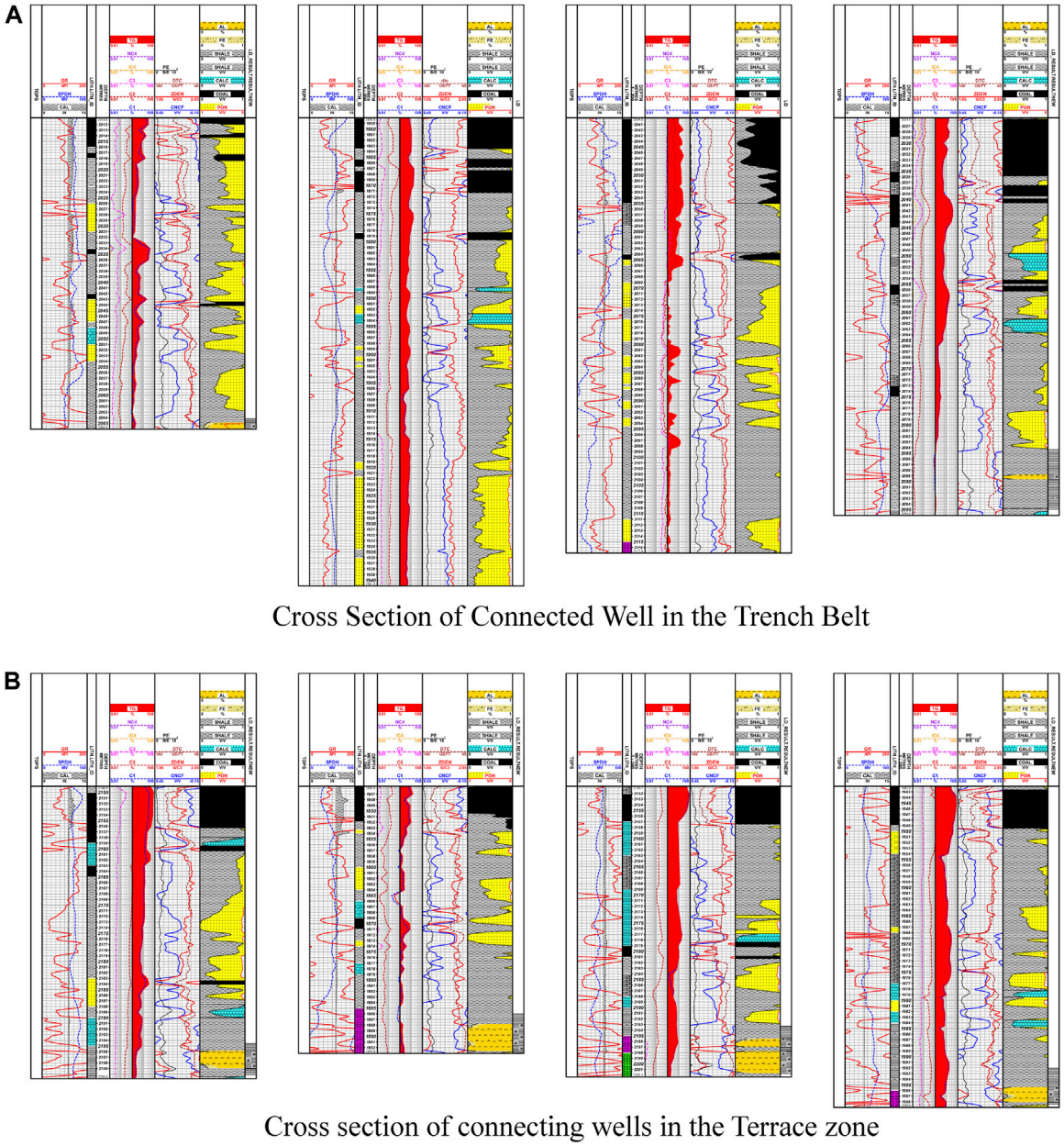

FIGURE 4
Analysis of logging interpretation and connected well profiles within different paleo-geomorphic units. **(A)** Cross section of connected well in the Trench Belt. **(B)** Cross section of connecting wells in the Terrace zone. **(C)** Cross section of connected wells in the in the sinkhole of monadnock. **(D)** Restoration map of paleo-geomorphology of benxi formation in region L Figure 4 Analysis of logging interpretation and connected well profiles within different paleo-geomorphic units.

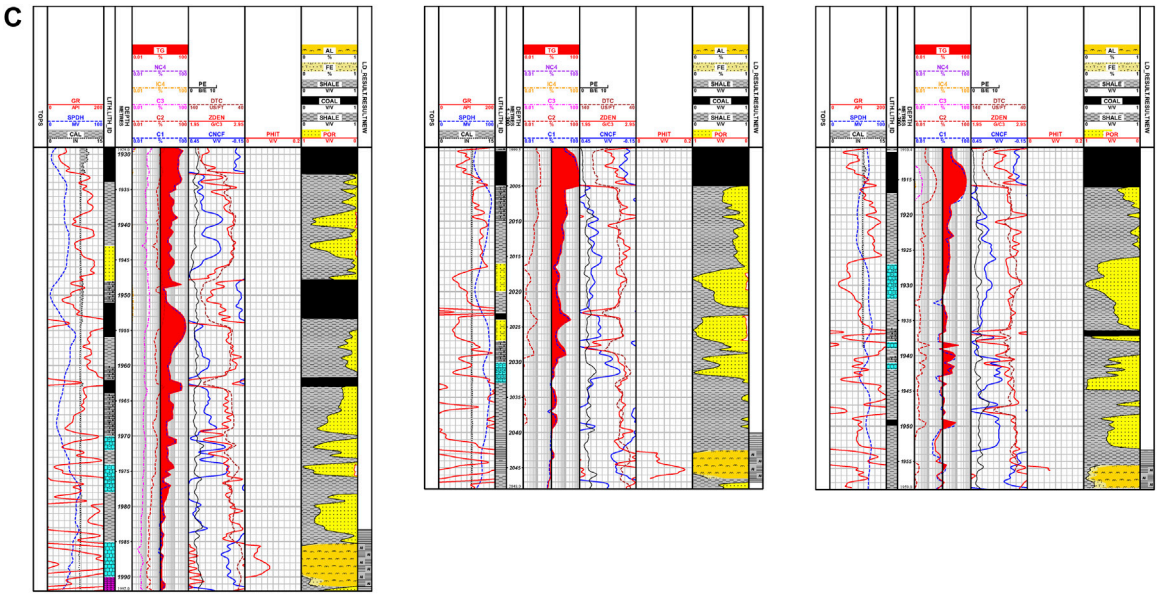

Cross section of connected wells in the in the sinkhole of monadnock

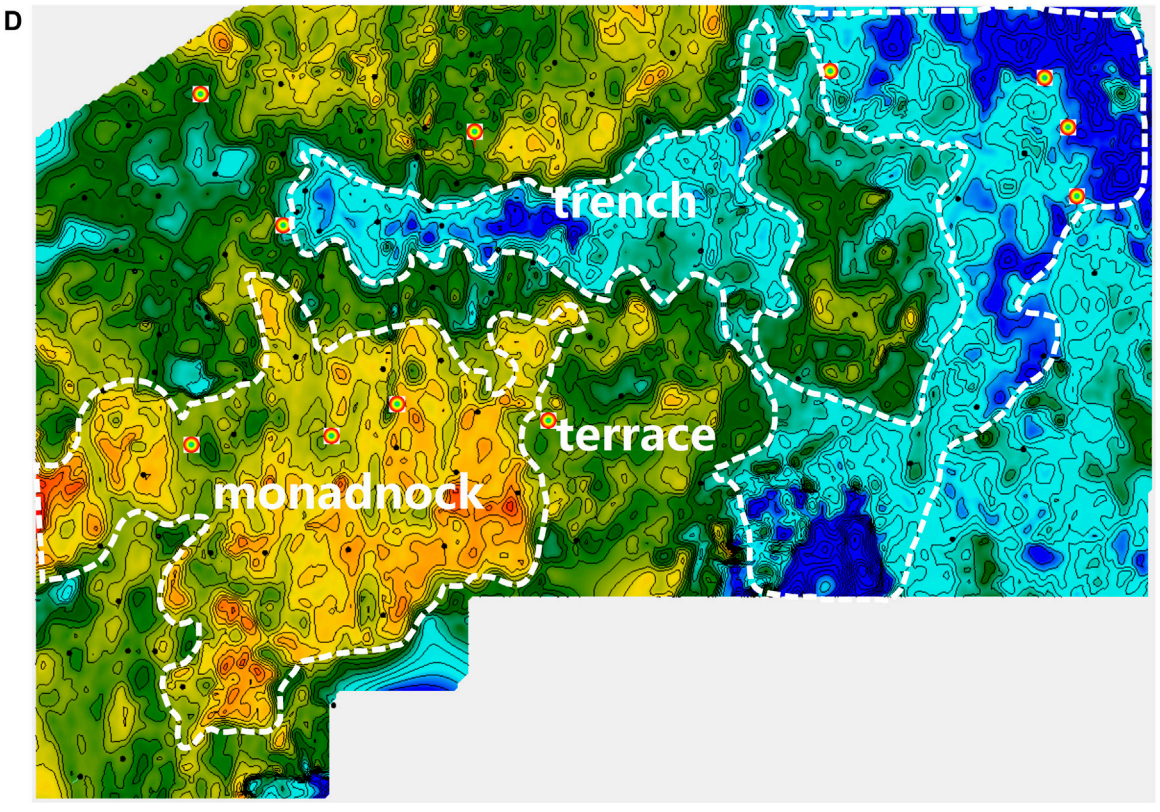

Restoration Map of paleo-geomorphology of Benxi Formation in Region L

FIGURE 4
(Continued) Analysis of logging interpretation and connected well profiles within different paleo-geomorphic units. **(A)** Cross section of connected well in the Trench Belt. **(B)** Cross section of connecting wells in the Terrace zone. **(C)** Cross section of connected wells in the in the sinkhole of monadnock. **(D)** Restoration map of paleo-geomorphology of benxi formation in region.

basins, and each secondary unit can be further divided into three levels of units. Conduct well connection analysis on the trench, monadnock, and terraces (slopes) within the third level unit, and summarize the impact of paleo-geomorphology units on the sedimentary thickness and porosity of bauxite.

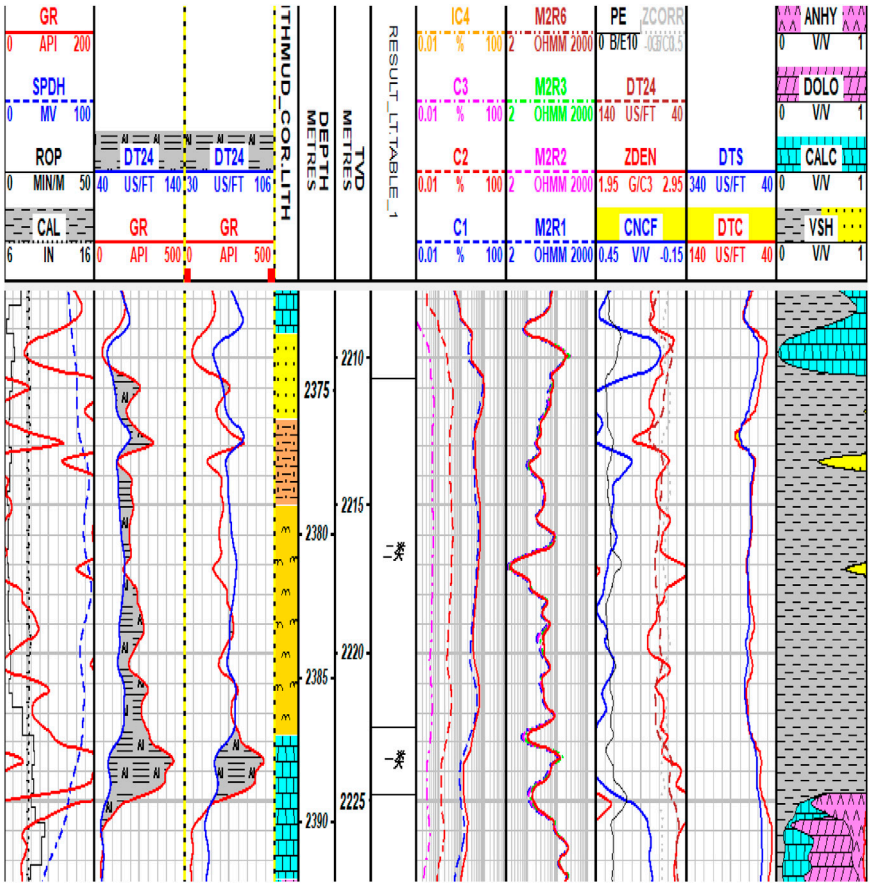

FIGURE 5
Qualitative analysis of logging interpretation.

Trench: As shown in Figure 4A, logging interpretation was performed on four wells within the trench, with a thickness range of 65–85 m for the Benxi Formation. Three wells are located in the trench zone of the basin, with bauxite rock thicknesses of 0, 0, and 0.7 m respectively; A well is located in a slope trench zone, with a thickness of 1.2 m of bauxite and an average thickness of about 0.5 m.

Slopes: As shown in Figure 4B, logging interpretation was performed on four wells within the slopes. The thickness range of the Benxi Formation for the four wells is 50.4–57 m, located in the slope zone. The thickness of the bauxite rock is 3.2, 4.8, 4.7, and 3 m, respectively, with an average thickness of 3.9 m.

Monadnock:As shown in Figure 4C, logging interpretation was performed on three wells with the sinkhole in the monadnock. The thickness range of the Benxi Formation in the three wells is 48.5–63 m, located in the sinkhole of the slope monadnock. The thickness of the bauxite rock is 6.3, 4, and 3.5 m, with an average thickness of 4.6 m.

As shown in Figure 4, by restoring the thickness of paleo-geomorphology, we divided different units, and the wells within each unit were statistically analyzed.Besides, the thickness of bauxite in the trench zone is thinner than that of slopes and monadnock, and there is basically no bauxite reservoirs in the trench. There is the thicker and more pure bauxite rocks in slopes and monadnock, with a thickness of 3–6.3 m. The total gas values of bauxite rocks in the slopes areas are higher than those in the sinkhole of monadnock, indicating better gas properties.

5 Well logging evaluation

The qualitative identification of bauxite rock lithology is relatively simple, as shown in Figure 5. The anomaly high value of Gamma Ray in bauxite formation is the standard for qualitative identification. In the early stage, the GR and DT curve in the logging series intersected (the second and third channels) to distinguish between bauxite mudstone and high-quality bauxite reservoir. This method can only provide qualitative conclusions and has a relatively large error, making it difficult to quantitatively evaluate the porosity of high-quality bauxite rocks.

5.1 Establishing a logging model

Based on core experimental data and logging curve information, we can establish the relationship between rock

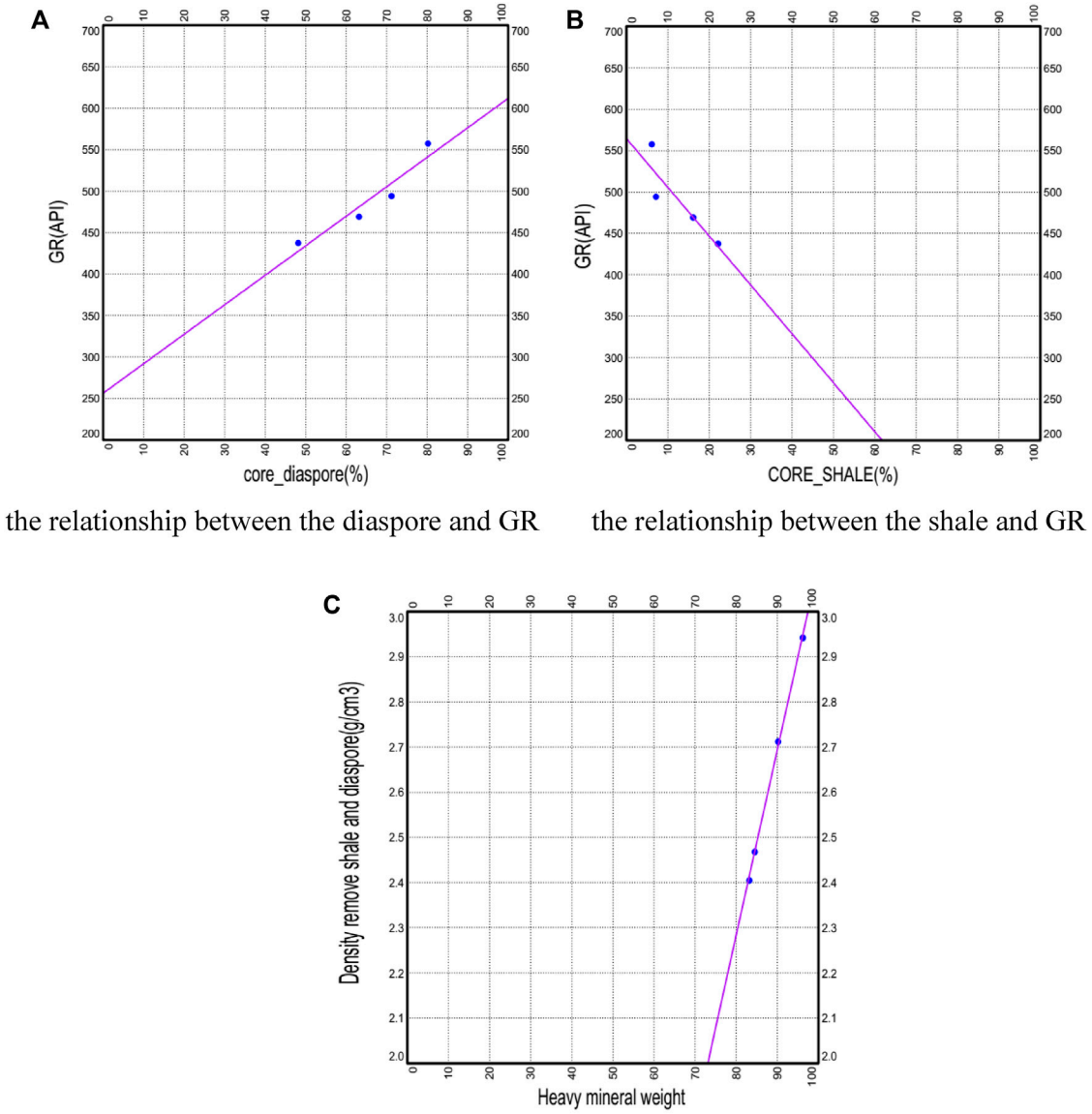

FIGURE 6
Relationship between mineral composition and logging response. **(A)** the relationship between the diaspore and GR. **(B)** the relationship between the shale and GR. **(C)** the relationship between the heavy mineral and density remove shale and diaspore.

mineral content and logging value, from formula 1–3. As shown in Figure 6, the R^2 is 0.996, 0.902, 0.998, respectively. And from these formulas we obtain a quantitative explanation of the lithological components. Based on the experience of neighboring areas, we establish the Wylle relationship between DT and porosity (equations 4; 5). And quantitatively explain the porosity of porosity and permeability through the pore permeability relationship.

$$V_{di} = 0.3717*GR - 114 \quad (1)$$

$$V_{py+an} = \frac{\rho + 1.0003 - 2.65*V_{sh} - 0.0411*V_{di}}{0.055485} \quad (2)$$

$$V_{sh} = -0.18823*GR + 104 \quad (3)$$

$$\Delta t_{ma} = 127.4V_{di} + 194V_{py+an} + 250V_{sh} \quad (4)$$

$$\varnothing = \frac{\Delta t - \Delta t_{ma}}{\Delta t_f - \Delta t_{ma}} - V_{sh}\frac{250 - \Delta t_{ma}}{\Delta t_f - \Delta t_{ma}} \quad (5)$$

5.2 Model validation

We verified the correctness of the quantitative lithology and porosity of the logging interpretation model through two wells, L-XX and L-XY. Among them, L-XX has core experimental data, and L-XY well has conducted NMR logging in the bauxite formation. Figure 7 is the log interpretation diagram of L-XX well. The logging traces from left to right in the figure are lithology logging traces, depth traces, total gas logging

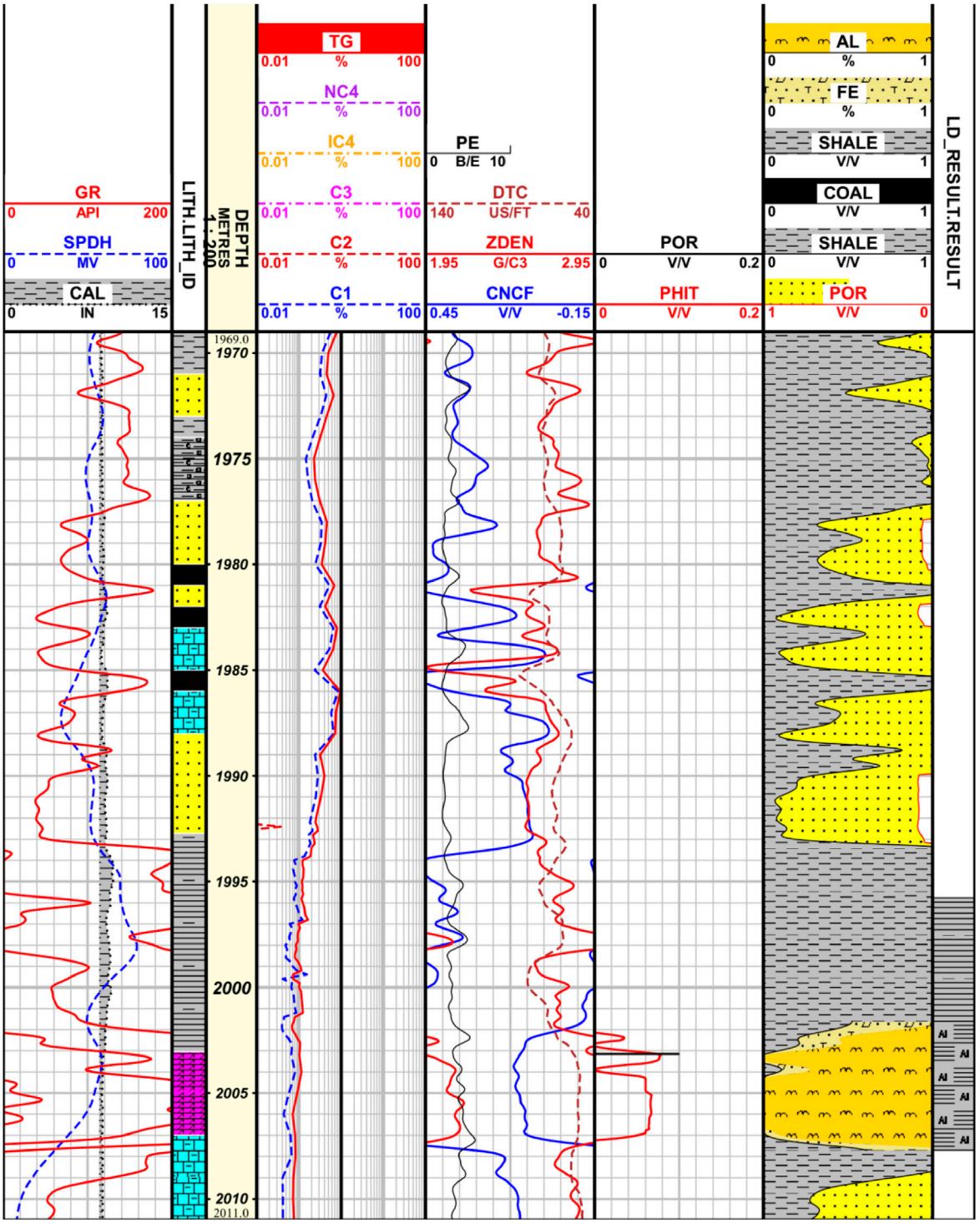

FIGURE 7
L-XX well logging interpretation and core experiment diagram.

traces, porosity logging traces, porosity traces, logging quantitative interpretation lithology traces, and logging interpretation conclusion traces. The content of diaspore, heavy mineral, and clay in the logging interpretation results of L-XX well is 94.5%, 1.1%, and 4.2%, respectively. Compared with the results of XRD diffraction analysis 94, 3, and 3, the relative errors are 0.5%, 1.9%, and 1.2%, respectively. Figure 8 is the log interpretation diagram of L-XY well. The porosity of the well was interpreted in sections ① and ②, which is consistent with the bimodal characteristics of the NMR T2 spectrum, verifying the rationality of quantitative interpretation of lithology and porosity.

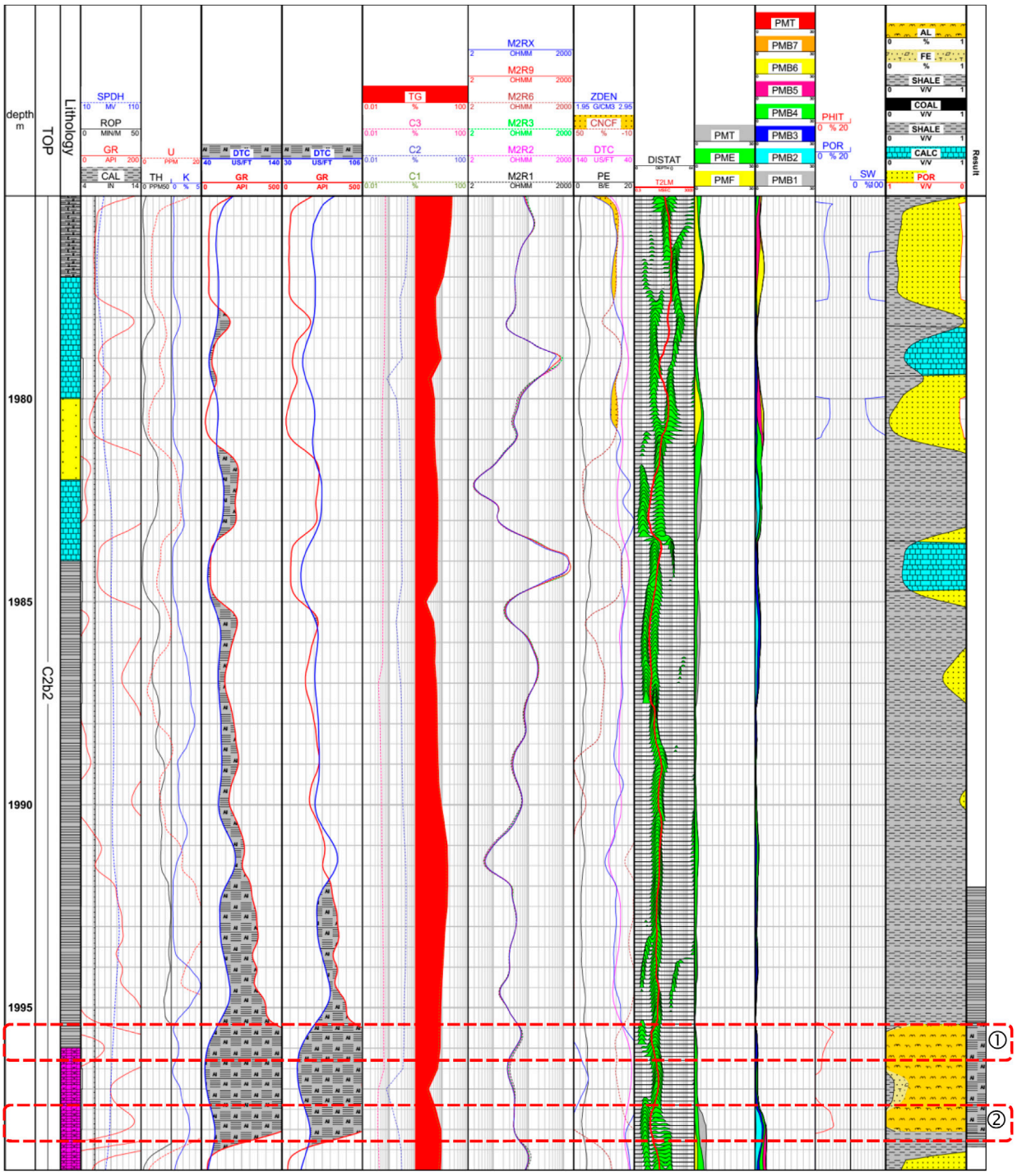

FIGURE 8
L-XY well logging interpretation of bauxite with NMR logging.

5.3 Imaging logging analysis

The imaging logging series includes various logging methods such as acoustic wave, resistivity, nuclear magnetic resonance, etc., (Wang et al., 2022; Wang et al., 2021; Dan et al., 2019). At present, the development of imaging logging has been able to quantitatively evaluate fractures, identify pore structures, and evaluate fluid properties (Wang et al., 2023; Li et al., 2021; Li et al., 2021; Ben et al., 2020; Yang et al., 2019). This study further analyzes the pore structure and fluid properties of bauxite strata through electrical imaging porosity spectrum, conductivity spectrum, and apparent formation water resistivity distribution spectrum. The 14th trace in

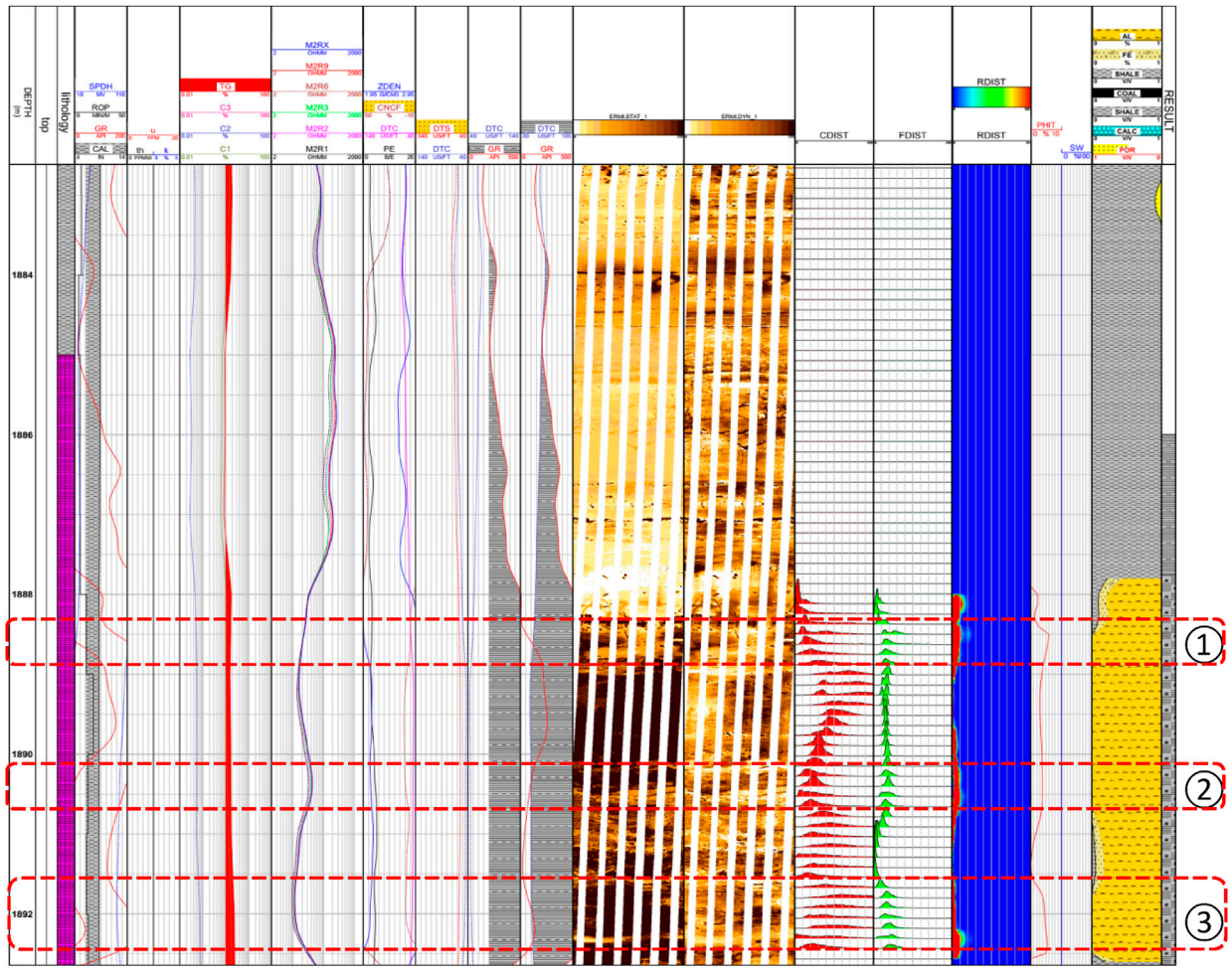

FIGURE 9
Analysis of electrical imaging logging spectrum.

Figure 9 shows the conductivity spectrum, which mainly reflects the difference in conductivity in the imaging logging image. In areas with high conductivity, the peak value shifts back as a whole. Both bauxite and argillaceous bauxite have high electrical conductivity. Conventional lithology analysis shows that some of the high electrical conductivity is influenced by heavy minerals and does not have good pores. The 15th trace in Figure 9 shows the porosity spectrum, which is similar to the T2 spectrum of NMR logging and can reflect the distribution of formation porosity and large and small pores. Compared with conventional lithology, it can be seen that bauxite with high content of diaspore has more developed pores. The developed porosity intervals in this well can be divided into three sections. There is a trailing phenomenon in the porosity spectrum, but the trailing is not obvious, indicating that the development degree of large pores is worse than that of ① and ③.The 16th trace in Figure 12 shows the distribution spectrum of apparent formation water resistivity, which can reflect the distribution of resistivity of fluids contained in the pores of the formation. The water layer has low resistivity and narrow spectral gaps. The gas layer has high resistivity and wide spectral peaks. The pore fluid in the bauxite rock of this well is mainly composed of water layers.

6 Conclusion

This article analyzes and processes seismic data and data from over 160 drilled wells, combined with core experimental data, to conduct a detailed analysis of bauxite reservoirs, and obtains the following understanding:

1) The bauxite strata in this region have been revealed through more than 160 drilled wells, and some of the wells have good reservoir properties and gas properties, making it a new type of unconventional reservoir. The average porosity of the drilled reservoirs in this favorable area is greater than 8%, which has certain exploration and development potential.
2) We completed the restoration of weathered crust paleo-geomorphology in the underlying strata of bauxite through the impression method. Based on the thickness of the drilled Benxi Formation, the second and third level units of paleo-geomorphology are divided. The thickness distribution of each third level unit of paleo-geomorphology is summarized, and the thickness of drilled bauxite is analyzed. It is believed that bauxite is distributed in sheet, strip, and point shapes in karst

monadnock, karst slopes or terraces, and karst trench, respectively. The lithology and porosity of bauxite rocks with different distributions are not the same.

3) The bauxite reservoir has special logging response characteristics, namely, high gamma, high density, high neutron, low resistance, and low difference time. It has a clastic structure and well-developed primary intergranular pore network. Through core experiments, a quantitative interpretation standard for bauxite rock was established for quantitative interpretation of lithology and porosity. The rationality of the interpretation was verified by combining imaging logging series, and further exploration was conducted on the pore structure and fluid properties of bauxite rock. The interpretation method of bauxite rock logging evaluation in this block was studied from scratch.

Data availability statement

The raw data supporting the conclusion of this article will be made available by the authors, without undue reservation.

Author contributions

QY: Writing–original draft, Writing–review and editing. LD: Writing–original draft, Writing–review and editing. YS: Writing–original draft, Writing–review and editing. LQ: Writing–original draft, Writing–review and editing.

Funding

The author(s) declare financial support was received for the research, authorship, and/or publication of this article. This research work has been supported by the technology project of China National Offshore Oil Corporation, titled “Reservoir Formation Conditions and Exploration Key Technologies for Bauxite and Ordovician in the Eastern Margin of the Ordos Basin” (No. KJZH-2023-2104).

Conflict of interest

Authors QY, LD, YS, and LQ were employed by Cnooc Research Institute Ltd.

The authors declare that this study received funding from China National Offshore Oil Corporation. The funder had the following involvement in the study: the study design, collection, analysis, interpretation of data, the writing of this article, and the decision to submit it for publication.

Publisher’s note

References

Ben, J. L., Qiao, W. X., Che, X. H., Ju, X. D., Lu, J. Q., and Men, B. Y., Field validation of imaging an adjacent borehole using scattered P-waves. *Petroleum Sci.*, 2020, 17, 1272–1280. doi:10.1007/s12182-020-00475-5

Cao, H., Wu, H., Ren, X., et al. (2020). Karst paleogeomorphology and reservoir distribution pattern of Ordovician in the southeastern Ordos Basin. *China Pet. Explor.* 25 (3), 146–155. doi:10.3969/j.issn.1672-7703.2020.03.013

Chen, Li, Sun, L., and Sun Hansen, E. (2022). A method to evaluated gas content with coalbed methane reservoir based on adsorption theory and production analysis. *Geofluids* 2022, 3558643. doi:10.1155/2022/3558643

Dan, L. I., Qiao, W., Che, X., et al. (2019). Study on the response of dipole reflected acoustic imaging the near-borehole cave. *J. Appl. Acoust.* 38 (5), 767–773. doi:10.11684/j.issn.1000-310X.2019.05.002

Du, G., Li, M., Yu, bo, et al. (2022). *Seismic prediction technology and application of Taiyuan Formation bauxite reservoir in Longdong area*. Hainan, China: The Geophysical Exploration Technology Seminar of the Chinese Petroleum Society.

FengRuyong, A. (2022). Method to improve computational efficiency of productivity evaluation with rectangular coalbed methane reservoir. *Geofluids* 2022, 7341886. doi:10.1155/2022/7341886

Fu, J., Li, M., Zhang, L., et al. Breakthrough in the exploration of bauxite gas reservoir in Longdong area of the Ordos Basin and its petroleum geological implications. *Nat. Gas. Ind.*, Vol. 41, 11, p. 1–11. 2021. doi:10.3787/j.issn.1000-0976.2021.11.001

Fu, J., Zhao, H., Guodong, DONG, et al. (2023). Discovery and prospect of oil and gas exploration in new areas of Ordos Basin. *Nat. Gas. Geosci.* 34 (8), 1289–1304. doi:10.11764/j.issn.1672-1926.2023.06.004

Jia, L., Liu, H., Xue, Y., et al. Paleo-geomorphology and Gas-water distribution law in Shaan X block on the east side of Jingbian gas field. *Sci. Technol. Eng.*, 2023, 23(12), 5022–5032. doi:10.3969/j.issn.1671-1815.2023.12.011

Jiang, J., and Wang, B., Natural gas generation and reserve in taiyuan group of low permian in east of Ordos Basin, *Nat. Gas. Geosci.*, 2004, 15(5), 511–515. doi:10.3969/j.issn.1672-1926.2004.05.014

Li, D. (2023). A three-dimensional display technology of reflected acoustic logging and its application example. *Geofluids* 2023, 7979348. doi:10.1155/2023/7979348

Li, D., Qiao, W. X., Che, X. H., Ju, X., Yang, S., Lu, J., et al. Eliminating the azimuth ambiguity in reflected S-wave imaging logging based on the azimuthal receiver mode. *J. Petroleum Sci. Eng.*, 2021, 199: 108295. doi:10.1016/j.petrol.2020.108295

Liu, W., Pan, H., Li, J., et al. Well logging evaluation on bauxitic mudstone reservoirs in the Daniudi Gasfield, Ordos Basin. *Nat. Gas. Ind.*, 35(5),24–30. 2015. doi:10.3787/j.issn.1000-0976.2015.05.004

Liu, D., Zhang, H., Yang, X., et al. Well logging evaluation of bauxite reservoirs in Ordos Basin.*Xinjiang Pet. Geol.*, 43(3),2022b:P261–P270. doi:10.7657/XJPG20220302

Liu, K., Fu, X., Rong, W., et al. (2022a). Analysis of bauxite reservior in X area of Ordos Basin. *J. Xi`an Shiyou Univ. Sci. Ed.* 37 (2), P25–P31. doi:10.3969/j.issn.1673-064X.2022.02.004

Nan, J., Liu, Na, Wang, X., et al. (2022). Characteristics and formation mechanism of bauxite reservoir in Taiyuan Formation,longdong area,Ordos Basin. *Nat. Gas. Geosci.* 33 (2), 288–296. doi:10.11764/j.issn.1672-1926.2021.11.008

Pan, Bo, Zhao, W., Liu, D., et al. Geochemical characteristics of bauxite deposits of Benxi Formation in shenmu-mizhi area,Ordos Basin. *Nat. Gas. Geosci.*, 2023, 34(6): 1072–1089. doi:10.11764/j.issn.1672-1926.2023.01.009

Qiu, Yu, Li, A., Zhou, J., et al. (2021). Calibrating the bottom interface of granite weathering crust reservoir on the Songnan lift in the deep water areas of Qiongdongnan Basin. *Mar. Geol. Front.* 37 (7), 87–96. doi:10.16028/j.1009-2722.2021.087

She, Y., Fei, Li, Wang, Y., et al. (2022). *High resolution inversion technology and application of bauxite reservoir in Qingcheng area of Ordos Basin*. Hainan, China: The Geophysical Exploration Technology Seminar of the Chinese Petroleum Society.

Tang, L., Song, Y., Chen, X., Jiang, Z., Zhang, F., Li, Q., et al. (2023). Key parameters and the upper-lower limits of shale gas selection evaluation: case study from the Wufeng-Longmaxi Formation in the Sichuan Basin. *Nat. Gas. Geosci.* 34 (1), 153–168. doi:10.11764/j.issn.1672-1926.2022.09.011

Tang, L., Song, Y., Zhao, Z., et al. (2022). Origin and evolution of overpressure in shale gas reservoirs of the upper ordovician wufeng formation–lower silurian longmaxi Formation in the sichuan basin. *Nat. Gas. Ind.* 42 (10), 48–64. doi:10.3787/j.issn.1000-0976.2022.10.004

Wang, S., Wang, G., Huang, L., Song, L., Zhang, Y., et al. (2021). Logging evaluation of lamina structure and reservoir quality in shale oil reservoir of Fengcheng Formation in Mahu Sag, China. *Mar. Petroleum Geol.* 133, 105299. doi:10.1016/j.marpetgeo.2021.105299

Wang, S., Wang, G., Lai, J., Liu, S., Chen, X., et al. (2020). Logging identification and evaluation of vertical zonation of buried hill in Cambrian dolomite reservoir: a study of Yingmai-Yaha buried hill structural belt, northern Tarim basin. *J. Petroleum Sci. Eng.* 195, 107758. doi:10.1016/j.petrol.2020.107758

Wang, S., Wang, G., Li, D., Wu, X. N., Chen, X., Wang, Q. Q., et al. (2022). Comparison between double caliper, imaging logs, and array sonic log for determining the *in-situ* stress direction: a case study from the ultra-deep fractured tight sandstone reservoirs, the Cretaceous Bashijiqike Formation in Keshen8 region of Kuqa depression, Tarim Basin, China. *Petroleum Sci.* 19 (6), 2601–2617. doi:10.1016/j.petsci.2022.08.035

Xu, C., Lai, W., Zhang, X., et al. (2023). New progress and future exploration thinking of CNOOC oil and gas exploration.*China Offshore Oil Gas*, 35 (2), 1–12. doi:10.11935/j.issn.1673-1506.2023.02.001

Yang, H., Xi, S., Wei, X., et al. Evolution and natural gas enrichment of multicycle superimposed basinin Ordos Basin. *Pet. Geol.*, 2006, 1, 17–24.

Yang, S. B., Qiao, W. X., and Che, X. H., Numerical simulation of acoustic field in logging-while-drilling borehole generated by linear phased array acoustic transmitter . *Geophys. J. Int.*, 2019, 217(2): 1080–1088. doi:10.1093/gji/ggz071

Yuan, Z., Wu, F. U.-li, and Rong, FENG.The distribution rule and its geological significance of Bauxite in Yanchang gasfield of Ordos Basin.*J. Xi`an Univ. Sci. Technol.*, 36(6), 2016: P843–P848. doi:10.13800/j.cnki.xakjdxxb.2016.0614

Zhu, G., Li, B., Li, Z., et al. (2022). Practices and development trend of unconvertional natural gas exploration in eastern margin of Ordos Basin:Taking Linxing-Shenfu gas field as an example. *China offshore Oil Gas* 34 (4), 16–29. doi:10.11935/j.issn.1673-1506.2022.04.002